Chapter 7

Amelioration of Blood Compatibility and Endothelialization of Polycaprolactone Substrates by Surface-Initiated Atom Transfer Radical Polymerization

Shaojun Yuan, Gordon Xiong, Ariel Roguin,
Swee Hin Teoh and Cleo Choong

Additional information is available at the end of the chapter

http://dx.doi.org/10.5772/52646

1. Introduction

Attempts to develop synthetic vascular grafts for the replacement of diseased vascular sections have been an area of active research over the past decades [1]. However, thrombosis formation as a result of platelet adhesion to the luminal surface of synthetic graft and restenosis caused by host inflammatory remain a challenge, especially for small-diameter (<6 mm) graft replacement [2,3]. Therefore, the haemocompatibility of the biomaterial used in the graft is a prerequisite for clinical success. As the result, various strategies have been developed to improve the blood compatibility of biomaterial surfaces, including the surface immobilization of anti-coagulants such as heparin [4] and sulfated silk fibroin [5], the incorporation of polyethylene oxide or negatively charged side chains [6,7], and surface passivation with protein layers, such as albumin [8]. Despite the efficacy of these approaches in preventing acute thrombogenesis, concerns remain on the drug elution lifespan, with possible consequence of late thrombosis [9]. To avoid undesirable blood-material interaction, the seeding of autologous endothelial cells (ECs) onto the luminal surface of the graft is considered to be an ideal approach to increase the patency of synthetic grafts [10]. Many studies have indicated that endothelial cells release factors that regulate thrombogenesis and platelet activation [11], while delayed or absent stent endothelialization has been implicated in late thrombosis and adverse clinical outcomes [13]. Thus, rapid endothelialization of vascular grafts is of great importance for blood-contacting vessels for long-term patency.

Due to its slow degradation rates in vivo (2-4 years) [14], good mechanical strength, and biocompatibility with vascular cell types [15,16], polycaprolactone (PCL) is currently being ex-

tensively investigated as scaffolds for vascular tissue engineering applications [17-21]. However, the intrinsic hydrophobicity and poor cytocompatibility of PCL substrates lead to poor affinity for cell adhesion, thereby restricting their applications as blood-contacting devices. Consequently, surface modification of PCL is necessary to improve cell adhesion and proliferation. Functional polymer brushes containing reactive hydroxyl (-OH), carboxyl (-COOH) or amine (-NH2) groups have been successfully grafted onto the PCL surfaces using γ-ray irradiated, ozone or photo-induced polymerization grafting to introduce hydrophilicity [9,16,22-24]. These flexible reactive groups on the polymer brushes are well-suited to conjugate bioactive macromolecules for improved cytocompatibility. However, γ-ray irradiated, ozone or photo-induced polymerization grafting of polymer brushes has several limitations, including low density of grafting due to steric hindrance, uncontrollable graft yield of polymer brushes, and undesired formation of a covalent bond between reactive groups on the polymer brushes and the surface [25]. Hence, an alternative grafting approach that allows control over brush density, polydispersity and composition is desired.

One such alternative is the use of surface-initiated atom transfer radical polymerization (ATRP) approach to covalently graft polymer brushes in a tunable and controllable manner [26]. This approach allows the preparation of well-defined dense polymer brushes containing reactive pendant groups (e.g. -OH, -COOH, or epoxide groups), and provides highly reactive binding sites for functional biomolecules.[27] As a result, surface-initiated ATRP provides a promising approach to fabricate PCL substrates with well-defined polymer brushes of controlled length and density, as well as tunable grafting density of biomacromolecules. However, to the best of our knowledge, only few studies have been devoted to modifying biodegradable polyester polymers using surface-initiated ATRP to improve their cytocompatibility or blood compatibility [27,28]. Also, the functionality of the attached cells was not thoroughly investigated in those studies.

As such, the aim of the current study is to utilize the surface-initiated ATRP method to tailor PCL substrates with dense functional P(GMA) brushes and high-density immobilized gelatin to improve their properties for cell attachment and proliferation. Each functionalization step was ascertained by XPS, AFM and water contact angle measurements. The cytocompatibility of the functionalized PCL substrates was evaluated using human umbilical vein endothelial cells (HUVECs) and the effect of different surface properties on the regulation of the thrombogenicity of the attached cells was also investigated.

2. Materials and methods

2.1. Materials

Polycaprolactone pellets (PCL, average M_n45000), 1,6-hexanediamine (98%), glycidyl methacrylate (GMA, >97%), 2-bromoisobutyrl bromide (BIBB, 98%), 2,2'-bipyridine (bpy, 98%), dichloromethane (anhydrous, >99.8%), triethylamine (TEA, 98%), isopropyl alcohol, hexane (anhydrous, >95%), copper (I) bromide (CuBr, 99%), copper (II) bromide ($CuBr_2$, 98%), and gelatin (Porcine skin, Type A) were obtained from Sigma-Aldrich Chemical Co. (St. Louis,

http://dx.doi.org/10.5772/52646

MO, USA), and were used without further purification. GMA was passed through a silica gel column to remove the inhibitor, and stored under a nitrogen atmosphere at -4°C. All the other chemical reagents and solvents were used as received. Human Umbilical Vein Endothelial cells (HUVECs, ATCC CRL-1730™) were purchased from American Type Culture Collection (Manassas, VA, USA). Cell culture medium (MCDB131), heparin and paraformaldehyde (4%, v/v) were obtained from Sigma-Aldrich Chemical Co. Medium supplements, such as Foetal Bovine Serum (FBS), penicillin, amphotericin, bovine brain extract, streptomycin, and Trypsin-EDTA (0.25%), were purchased from Life Technologies (Carlsbad, CA, USA). LIVE/DEAD® cell viability assay reagent, AlamarBlue™ reagent, tissue thromboplastin (human brain extract), ellagic acid, and DAF-FM Diacetatewere obtained from Life Technologies. The P-selectin assay reagents were obtained from Serotec Co. (Kidlington, Oxford, UK).

2.2. Aminolysis of PCL film substrates and immobilization of ATRP initiator

Polycaprolactone (PCL) films were prepared by solution casting method using previously established methods [29]. Briefly, 5 g of the PCL pellets was dissolved in 40 ml of dichloromethane to form the PCL solution. The polymer solution was then cast onto the glass substrate with predetermined thickness using the automatic film applicator (PA-2105, BYK). The solvent was removed at room temperature by slow evaporation over a 24 h period, and was further dried in a vacuum oven for another 24 h at 35 °C to obtain the translucent PCL films with a thickness of about 150 μm. The resultant PCL films were cut into round-shaped specimens with a diameter of 2 cm. The activation of PCL substrates was performed by aminolysis treatment using a procedure previously described [30,31]. Briefly, the PCL films were immersed in a 10% (w/w) 1,6-hexanediamine and isopropanol mixture at 40 °C for a predetermined time. After aminolysis treatment, the resultant PCL-NH_2 surfaces were thoroughly rinsed with copious amounts of deionized water and isopropanol, respectively, to remove free 1,6-hexanediamine, and dried in a vacuum oven at 30 °C for 24 h.

The introduction of an alkyl halide ATRP initiator on the PCL-NH_2 surface was accomplished through the reaction of the amino groups with 2-bromoisobutyrate bromide (BIBB) [32]. The PCL-NH_2 films were immersed in 30 ml of anhydrous hexane solution containing 1.0 ml (7.2 mmol) of triethylamine (TEA). After 30 min of degassing with nitrogen, the reaction mixture was cooled in an ice bath, and 0.89 ml (1.65g, 7.2 mmol) of BIBB was added dropwise via a syringe. The reaction was allowed to proceed with gentle stirring at 0 °C for 2 h and then at room temperature for 12 h. The resulting surface (referred to as the PCL-Br surface) was washed thoroughly with copious amounts of hexane, ethanol, and finally deionized water, in that order, and was subsequently dried in a vacuum oven under reduced pressure at ambient temperature overnight.

2.3. Surface-initiated ATRP of GMA and immobilization of gelatin

For the grafting of P(GMA) brushes from the PCL-Br surfaces, surface-initiated ATRP of GMA was performed using a [GMA (3 ml)]:[CuBr]:[$CuBr_2$]:[Bpy] molar feed ratio of 100:1.0:0.2:2.0 in 5 ml of methanol/water mixture (5/1, v/v) at room temperature in a Pyrex® tube. The reaction was allowed to proceed for 0.5 to 3 h to produce the PCL-*g*-P(GMA) sur-

faces. After the prescribed reaction time, the films were removed and washed sequentially with copious amount of methanol and deionized water, followed by immersing in methanol for about 48 h to ensure the complete removal of the physically-adsorbed reactants or polymers. For the immobilization of gelatin onto the pendant epoxide groups of the P(GMA) brushes, the PCL-*g*-P(GMA) films were incubated in 10 ml of the phosphate buffered saline (PBS, pH 7.4) containing 3 mg/ml gelatin. The reaction was allowed to proceed at room temperature for 24 h under continuous stirring to produce the corresponding PCL-*g*-P(GMA)-*c*-gelatin surfaces. After the reaction, the gelatin-immobilized PCL films were washed thoroughly with PBS solution and deionized water to remove the physically adsorbed (reversibly-bound) gelatin, prior to being dried in a vacuum oven under reduced pressure overnight.

2.4. Grafting density of the P(GMA) brushes and immobilized gelatin

The grafting density of the P(GMA) brushes and the amount of immobilized gelatin on the PCL substrates was determined by the grafting yield (GY) using the following equation [27,33]:

$$GY = \frac{W_a - W_b}{A} \tag{1}$$

Where Wa and Wb are the weights of the dry film after and before graft polymerization (or immobilization of gelatin) respectively, and A is the film area (about 3.2 cm^2). For each GY measurement, a minimum of three pieces of PCL films was used and the resulting values were averaged.

2.5. Surface characterization

The composition of the functionalized PCL films was determined by X-ray photoelectron spectroscopy (XPS). All the XPS spectra were recorded on a Krato AXIS Hsi spectrometer with a monochromatic Al Kα X-ray source (1486.6 eV photons), using procedures similar to those described previously [32]. The N 1s core-level signal can be used as an indicator of the immobilized gelatin. The [N]/[C] ratio, as determined from the sensitivity-factor-corrected N 1s and C 1s core-level XPS spectral area, indicated the relative abundance of the immobilized gelatin on the PCL substrates. Static water contact angles of the functionalized PCL film surfaces were measured at 25 ^oC and 60% relative humidity using a sessile drop method with 3 μl water droplets on a FTÅ 200 contact angle goniometer (First Ten Angstroms Inc., Portsmouth, VA, USA). The contact angles reported were the mean values from four substrates, with the value of each substrate obtained by averaging the contact angles for at least three surface locations. The surface topography of the functionalized PCL substrates was investigated by atomic force microscope (AFM). A multimode scanning probe microscope equipped with a NanoscopeIIIa controller (Digital Instrument, Santa Barbara, USA) was used to capture the AFM images in air. 10 μm scans were recorded in tapping mode with a

http://dx.doi.org/10.5772/52646

silicon cantilever. The drive amplitude was about 300 mV, and the scan rate was between 0.5 and 1.0 Hz. The arithmetic mean of the surface roughness (R_a) was determined by Nanoscope software.

2.6. Cytocompatibility of the functionalized PCL substrates

Human umbilical vein endothelial cells (HUVECs, ATCC CRL-1730™) were cultured in gelatin-coated T25 flasks containing MCDB131 cell culture medium supplemented with Foetal Bovine Serum, 0.2% Bovine Brain Extract, 0.25 ug/ml amphotericin, 0.1 mg/ml heparin, 100 U/ml penicillin, and 100 ug/ml streptomycin, in a CO_2 environment at 37°C. The MCDB131 medium was changed every other day. Upon 90% culture confluency, cells were harvested by trypsinization using 0.25% Trypsin-EDTA. ECs between 4-6 passages were used for subsequent experiments.

2.6.1. Cell proliferation

The pristine and functionalized PCL films were sterilized by immersing into 75% (v/v) ethanol solution for 60 min, and then rinsed thrice with sterile PBS, followed by MCDB131 medium incubation overnight. Gelatin-coated coverslips (0.1%) were used as positive controls. Cell viability and proliferation was determined using the AlamarBlue™(AB) assay. 0.5 ml of EC cell suspension (2×10^4 cells/ml) was seeded into each well of 24-well plate containing the pristine and functionalized PCL films, and incubated in a 5% CO_2 environment at 37 °C for 1, 3, 5 and 7 days. The cell culture medium was changed every other day. After the predetermined incubation period, culture media was removed from the wells, and 0.5 ml of the AB solution (10% AB solution in culture media without FBS) was added to the wells. The plates were incubated in a 5% CO_2 atmosphere at 37°C for 4 h and the fluorescence density was measured using a microplate reader (Model 680, Bio-Rad Laboratories, Inc. Hercules, CA, USA) at an excitation wavelength of 570 nm and an emission wavelength of 580 nm. Cell numbers were calculated using standards derived from seeding known quantities of cells and correlating with fluorescence emission.

2.6.2. Cell imaging

In vitro qualitative analysis of cell coverage and viability was performed using a LIVE/DEAD® viability/cytotoxicity assay to assess the extent of endothelialization on the functionalized PCL surfaces. For this procedure, calcein AM (4 mM in anhydrous dimethyl sulfoxide, DMSO) and EthD-1 (2 mM in DMSO/H2O, 1:4 v:v) were added to PBS (1:1000 ratio) to produce a LIVE/DEAD® staining solution. The cell-seeded PCL samples, obtained after 7 days cell culture, were first washed thrice with PBS to eliminate the nonadherent cells, followed by staining using 0.1 ml of LIVE/DEAD staining solution. After incubation in a 5% CO_2 atmosphere at 37°C for 30 min, the samples were visualized by Nikon Image Ti fluorescence microscope (emission at 515 nm and 635 nm (Nikon Instruments, Tokyo, Japan) to acquire fluorescent images using NIS-Elements Br software.

2.7. Blood compatibility of the bare and endothelialized PCL substrates

The hemolysis rate, coagulant activity, nitric oxide (NO) production, and platelet activation of the bare and endothelialized PCL films with various surface functionalizations were investigated to evaluate their blood compatibility. The endothelialized PCL substrates were obtained by culturing ECs (2×10^4 cells/ml) for 7 days on surface-functionalized PCL films using the procedures described above.

2.7.1. Hemolysis rate test

The pristine and functionalized PCL samples were immersed in diluted blood solution containing 2% fresh anticoagulated (ACD) human blood and 98% physiological salt solution and incubated at 37o for 1 h. After centrifugation at 3000 rpm for 5 min, the absorbance of solution was recorded as D_t. Under the same conditions, the solution containing 2% ACD blood and 98% physiological salt solution was used as a negative reference, and the solution containing 2% ACD blood and 98% distilled water was used as a positive reference. These absorbances were recorded as D_{nc} and D_{pc}, respectively. The hymolysis rate α of the samples was calculated using the following equation:

$$\alpha = \frac{D_t - D_{nc}}{D_{pc} - D_{nc}} \times 100\% \quad (2)$$

2.7.2. Coagulation assays

Whole blood of healthy human volunteers was mixed with 3.8% sodium citrate at a volume ratio of 1:9. The blood was centrifuged at 3000 rpm for 15 min at room temperature to obtain platelet-poor plasma (PPP). Aliquots of 500 μl of PPP were added to be in contact with the surfaces of each bare or endothelialized PCL substrate for 10 min at 37°C. The PPP was then collected and added with tissue thromboplastin (human brain extract) for prothrombin time (PT) tests, or added with a partial thromboplastin reagent (ellagic acid) for activated partial thromboplastin time (APTT) test. Subsequently, the fibrin clot formation time was determined by an automatic coagulation analyzer (Sysmex CA-7000). PPP that was not exposed to the PCL substrates was used as a blank sample.

2.7.3. Nitric Oxide (NO) secretion by HUVEC

ECs cultured for 7 days on the functionalized PCL substrates were washed twice with PBS and incubated at 37°C with trypsin-EDTA (0.25%) solution for cell detachment. The resultant ECs were serum-starved overnight in serum-free medium. After incubation with fresh serum-free medium for 6 h, the medium was removed and DAF-FM diacetate (Molecular Probes, D-23842) was added to the medium to effect a final concentration of 10 μM.The medium was subsequently incubated at 37 °C for 1 h, followed by detection of fluorescence using Glomax 20/20 luminometer equipped with a blue fluorescent module. The end product of DAF-FM diacetate and NO is a benzotriazole derivative with a fluorescence excitation

http://dx.doi.org/10.5772/52646

and emission maxima of 495 and 515 nm, respectively. Fluorescence units were normalized to cell numbers.

2.7.4. Platelet activation determination by P-selectinassay

Platelet activation by the bare and endothelialized PCL substrates was investigated using the P-selectin (CD62P) assay. Briefly, 100 μl of fresh human platelet rich plasma (PRP) was incubated with the bare or 7-day endothelialized PCL substrates at 37°C for 2 h. At the end of incubation, the films were thoroughly with copious amounts of PBS solution thrice, followed by adding 40 μl of anti-CD62P (1:100, v:v) to each film, and then incubated at 37°C for 1 h. After being washed thrice with PBS solution, the films were each incubated with 40 μl of horseradish peroxidase-conjugated sheep anti-mouse polycolonal antibody at 1:100 (v:v) at 37°C for 1 h. Subsequently, the PCL films were reacted with 150 μl of 3,3',5, 5'-tetramethylbenzidine (TMB) chromogenic solution for 10 min. The color reaction was terminated by adding of 100 μL of 1 M H_2SO_4, and the optical densities (OD) were measured at 450 nm using a Varioskan Flash Microplate Reader (Thermo Fisher Scientific, Waltham, MA, USA).

2.7.5. Gene and protein expression of vWF and activity of MMP-2 in ECs cultured on functionalized PCL surfaces

For the real-time qPCR of von Willebrand factor (vWF) and matrix metalloproteinase-2 (MMP-2), the total RNA was extracted from the ECs after 7 days in culture, reverse-transcribed into cDNA and analyzed as described above. The expression of vWF and MMP-2 was normalized to the housekeeping ribosomal protein L27 (rpl27). Endothelial cells treated with 10 ng /ml TNF were used as positive controls.

For the immunoblot detection of vWF protein, cells were lyzed in protein lysis buffer (0.1% sodium dodecyl sulfate, 0.5% triton X-100, and 0.5% sodium deoxycholate dissolved in pH 7.4 PBS) and resolved using a denaturing 10% SDS-PAGE. The proteins were then blotted onto a nitrocellulose membrane and after blocking with 5% non-fat milk in tris-buffered saline with 0.1% Tween (TBS-T), the membrane stained using a rabbit anti-human vWF antibody at 1:5000 and subsequently with anti-rabbit HRP-conjugated antibody at 1:10,000 in TBS-T. The vWF was then visualized after developing using chemiluminescence on X-ray film. For determination of the MMP-2 activity, proteins were extracted from trypsinized cells using the protein lysis buffer before resolving by electrophoresis through a 10% SDS-PAGE copolymerized with 0.1% gelatin as substrate for enzymatic digestion. The molecular sizes of gelatinolytic activities were determined using protein standards (Fermentas, Prestained PAGE rulers). Upon completion of gel running, the gel was incubated with 100 mL renaturation buffer containing 2.5% triton X-100 for 1 h at room temperature with agitation. The gel was subsequently incubated in 100 ml of development buffer containing 50 mM Tris base, 200 mM NaCl, 5 mM CaCl2, and 0.02% Brij-35 overnight at 37 °C. Developed gel was then stained by the Coomassie Blue and gelatinolytic activities of MMP-2 were determined by the transparent bands appeared at the molecular weight of approximately 68 kDa and 98 kDa, respectively.

2.8. Statistical analysis

Each experiment was carried out with four replicates (n = 4), and the data are presented as mean ± standard deviation (SD) unless of otherwise stated. Statistical analysis was carried out by means of one-way analysis of variance (ANOVA) with Tukey's post hoc test. The confidence levels of 95% ($p<0.05$) and 99% ($p<0.01$) were used and no adjustments were made for multiple comparisons.

3. Results and discussion

Polycaprolactone (PCL) films with gelatin-coupled poly(glycidyl methacrylate) (P(GMA)) brushes were prepared via the following reaction sequence (Fig. 1): (a) active amine groups were introduced to the PCL film surfaces by the aminolysis reaction, (b) the immobilization of an alkyl bromide ATRP initiator was achieved via TEA-catalyzed condensation reaction between the amine groups on the aminolyzed PCL substrates and 2-bromoisobutyryl bromide (BIBB), (c) well-defined P(GMA) functional brushes were covalently grafted from the ATRP initiator-immobilized PCL surface via surface-initiated ATRP of GMA, (d) cell-adhesive gelatin was directly coupled to the pendant active epoxide groups of the grafted P(GMA). Details of each functionalization step are discussed below.

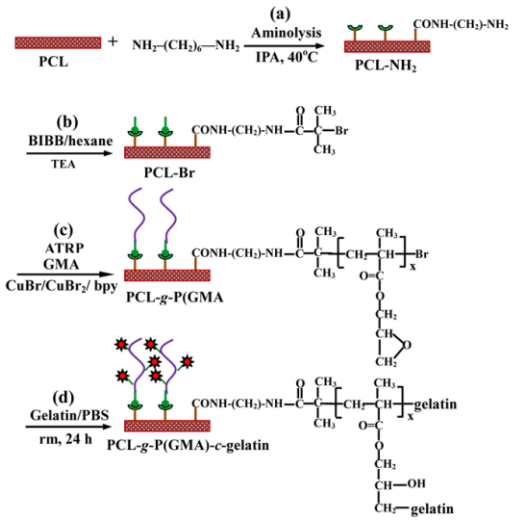

Figure 1. Schematic illustration of the process of (a) aminolysis of PCL substrates to introduce the free amino groups (the PCL-NH_2 surface), (b) immobilization of a alkyl bromine-containing initiator via condensation reaction to give the PCL-Br surface, (c) surface-initiated atom transfer radical polymerization (ATRP) of GMA from the PCL-Br surface to produce the PCL-*g*-P(GMA) surface, and (d) subsequently covalent conjugation of gelatin to obtain the PCL-*g*-P(GMA)-*c*-gelatin surface.

http://dx.doi.org/10.5772/52646

3.1. Aminolysis of PCL substrates and immobilization of ATRP initiator

Aminolysis represents an easy-to-perform chemical technique to engraft amino groups along the polyester chains, and hence has been widely used in the surface modification of scaffolds for tissue engineering applications [31,34]. In this study, PCL substrates were activated by the aminolysis reaction to introduce active amine groups. The relative amount of amine groups on the aminolyzed PCL (defined as the PCL-NH_2) surface was quantitatively determined by XPS measurements. The [N]/[C] ratio, as determined from sensitivity factor-corrected N 1s and C 1s core-level XPS spectral area, increases with the aminolysis time and reaches the maximal value after 1 h, which is estimated to be about 0.043 (Figs. 2). The result is consistent with the data reported previously [35,36]. As a degradation reaction, the aminolysis reaction is found to proceed preferentially at the amorphous regions of polymer in diamine solution during the initial period [37]. At longer aminolysis time, the decrease in bound amine groups may be caused by chain scission, formation of oligomers and other low mass fragments that are removed from the surface during reaction and the rinsing process [38]. Thus, the optimal aminolysis time for PCL film was found to be 1 h, and this reaction time was chosen for the subsequent surface modification and cell studies.

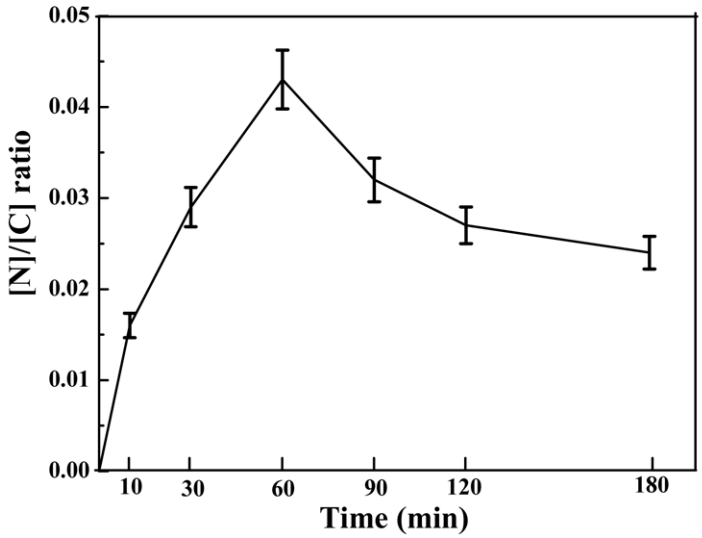

Figure 2. The [N]/[C] ratio of the aminolyzed PCL surface as a function of aminolysis time determined by XPS measurements. The analysis reaction of PCL films proceeded at 40°C in 10 wt% 1,6-hexanediamine/2-propanol solution. Error bars represent the standard deviation over separate measurement on three PCL films. The optimized aminolysis time was observed at 1 h with the [N]/[C] ratio of 0.043.

The chemical composition of the PCL film surfaces at various stages of surface modification was ascertained by XPS. Figs. 3a-3c show the respective wide scan, C 1s, and N 1s core-level spectra of the pristine PCL and PCL-NH_2 surfaces from 1 h of aminolysis. The C 1s core-level spectra of the pristine PCL can be curve-fitted into three peak components with binding

energies (BEs) at about 284.6, 286.2 and 288.7 eV, attributable to the C-H, C-O, and O=C-O species, respectively (Fig. 3b) [39]. The area ratio of [C-H]:[C-O]:[O=C-O] is around 5.0:1.1:1.0 (Table 1), which is in good agreement with the theoretical value of 5:1:1 for the polycaprolactone structures. The appearance of N 1s signal in the wide scan spectrum (Fig. 3a) and an additional peak component at 285.5 eV, attributable to C-N species, in the curve-fitted C 1s core-level spectrum (Fig. 3c) indicate the successful introduction of amine groups onto the PCL substrates after 1 h of aminolysis. The only peak component found at the BE of 399.6 eV in the N 1s core-level spectrum is associated with the free amine group on the PCL-NH_2 film surface (Fig. 3c') [38]. The decrease in static water contact angles of the PCL substrates from 93 ± 2° to 66 ± 3° is consistent with the presence of amine groups on the PCL-NH_2 surface (Table 1). The amine groups on the aminolyzed PCL surface can not only improve surface hydrophilicity, but also offer the active sites for further functionalization.

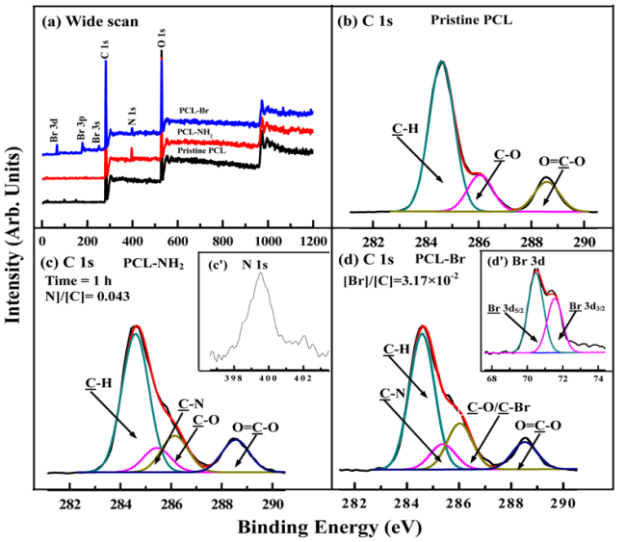

Figure 3. Wide scan and C 1s core-level curve-fitted XPS spectra of the (a,b) pristine PCL, (c,d) PCL-NH_2 from 1 h of aminolysis, and (e,f) PCL-Br surfaces. Insets of (d') and (f') correspond to the N 1s and Br 3d core-level XPS spectra of the PCL-NH_2 and PCL-Br surfaces, respectively.

The immobilization of a uniform monolayer of initiators on the solid surface is indispensible in the surface-initiated ATRP process [40]. An alkyl bromide ATRP initiator was introduced onto the PCL-NH_2 surface via TEA-catalyzed condensation reaction to produce the PCL-Br surface. Successful introduction of the alkyl bromide-containing ATRP initiator onto the PCL substrates can be deduced from the appearance of three additional signals with BEs at about 70, 189 and 256 eV, attributable to Br 3d, Br 3p, and Br 3s, respectively, in the wide scan spectrum of the PCL-Br surface (Fig. 3a) [41]. The [Br]/[C] ratio, as determined from the Br 3d and C 1s core-level spectral area ratio, was about 3.17×10^{-2} (Fig. 3d). The corresponding Br 3d core-level spectrum of the PCL-Br surface with a Br $3d_{5/2}$ BE of 70.4 eV is consistent

http://dx.doi.org/10.5772/52646

with the presence of the alkyl bromide species [41] (Fig. 3d'). The alkyl bromide-immobilized PCL surface became more hydrophobic, as static water contact angle increased noticeably to 85 ± 3° (Table 1).

Sample	GY[g](μg/cm²) (mean± SD[h])	[Br]/[C][i]	[N]/[C][i]	Surface composition[j] (molar ratio)	WCAk (degree)
Pristine PCL[a]	–	–	–	[C-H]:[C-O]:[O=C-O] = 5:1.1:1.0 (5:1:1)	93±2
PCL-NH_2 [b]	–	–	0.043	[C-H]:[C-N]:[C-O]:[O=C-O] = 4.7:0.7:1.1:1.0	66±3
PCL-Br[c]	–	3.17×10^{-2}	–	[C-H]:[C-N]:[C-O/C-Br]:[O=C-O] = 5.0:0.9:1.7:1.0	85±3
PCL-*g*-P(GMA)1[d]	6.31±1.32	9.29×10^{-3}	–	[C-H]:[C-O]:[O=C-O] = 3.8:2.8:1.0 (3:3:1)	62±4
PCL-*g*-P(GMA)2[e]	14.76±2.63	4.72×10^{-3}	–	[C-H]:[C-O]:[O=C-O] = 3.1:3.0:1.0 (3:3:1)	61±5
PCL-*g*-P(GMA)1-*c*-gelatin[f]	2.63± 0.52	–	0.169	[C-H]:[C-N]:[C-O]:[O=CNH]: [O=C-O] = 3.5:1.5:1.7:1.0:0.7	37±3
PCL-*g*-P(GMA)2-*c*-gelatin[pala]	3.79±0.73	–	0.203	[C-H]:[C-N]:[C-O]:[O=CNH]: [O=C-O] = 3.1:1.5:1.4:1.0:0.3	35±4

[a] Pristine PCL refers to the cleaned PCL film after rigorous wasing with alcohol/water solution and deionized water, [b] PCL-NH_2 was obtained after 1 h of aminolysis in a 10% (w/w) 1,6-hexanediamine/isopropanol solution at 40 °C, [c] PCL-Br was obtained after the PCL-NH_2 surface reacted with 2-bromoisobutyryl bromide (BIBB) in dried hexane containing 1:1 (molar ratio) BIBB and triehtylamine (TEA), [d,e] Reaction conditions: [GMA]:[CuBr]:[$CuBr_2$]:[bpy]=100:1:0.2:2 in methanol-water solution (1:1, v:v) at room temperature for 1 and 3 h to produce the PCL-*g*-P(GMA)1 and PCL-*g*-P(GMA)2 surfaces, respectively, [f] Reaction conditions: the PCL-*g*-P(GMA)1 and PCL-*g*-P(GMA)2 surfaces incubated in PBS (pH 7.4) solution containing the gelatin at a concentration of 3 mg/mL at room temperature for 24 h, [g] GY denotes the grafting yield, and is defined as GY = (W_a - W_b)/A, where W_a and W_b corresponds to the weight of the dry films before and after grafting of polymer brushes, respectively, and A is the film area (about 3.2 cm2
), [h] SD denotes standard deviation, [i] Determined from the corresponding sensitivity factor-corrected element core-level spectral area ratios, [j] Determined from the curve-fitted C 1s core-level spectra. Theoretical values are shown in parentheses. [k] WCA denotes static water contact angles.

Table 1. Grafting yield, surface composition, and water contact angles of the pristine PCL and surface-functionalized PCL surfaces

3.2. Surface-initiated ATRP of GMA and immobilization of gelatin

P(GMA) is an effective surface linker to immobilize biomolecules, such as proteins, antibodies or enzymes, for tissue engineering applications [42]. Fig. 4 shows the respective wide scan, C 1s and Br 3d core-level spectra of the PCL-*g*-P(GMA) surface from 1 and 3 h of ATRP reaction. The C 1s core-level spectra of the PCL-*g*-P(GMA) surface can be curve-fitted into three peak components with BEs at 284.6, 286.2 and 288. 7 eV, attributable to C-H, C-O and O=C-O, respectively (Figs. 4b and 4d). For the PCL-*g*-P(GMA)1 surface from 1 h of ATRP,

the area ratio of [C-H]:[C-O]:[O=C-O] is about 3.8:2.8:1.0 (Table 1), which is slightly different from the theoretical value of 3:3:1 for the GMA unit structure. The deviation in peak component area ratio of C 1s core-level spectrum of the PCL-g-P(GMA)1 surface suggests that the thickness of the P(GMA) brushes is less than the probing depth of XPS technique (about 8 nm in an organic matrix) [41]. Increasing the reaction time to 3 h leads to a [C-H]:[C-O]:[O=C-O] ratio of about 3.1:3.0:1.0, which is close to the theoretical value of the GMA repeat unit structure (Table 1). This is an indication that the P(GMA) brushes were thicker than the probing depth of XPS technique. It has been reported that the thickness of the P(GMA) brushes grafted on the silicon surface is around 30 nm after 3 h of ATRP of GMA under similar reaction conditions [41]. The presence of P(GMA) brushes leads to decrease in static water contact angles to 62 ± 4° and 61 ± 5°, respectively, for the PCL-*g*-P(GMA)1 and PCL-*g*-P(GMA)2 surfaces, owing to the presence of hydrophilic epoxide groups [43].

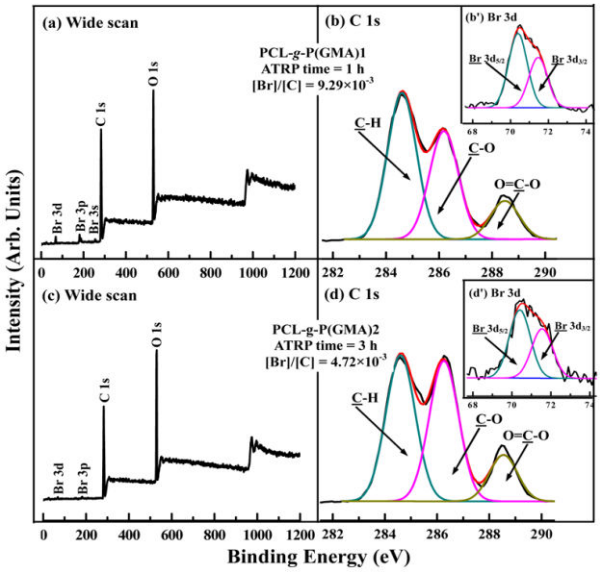

Figure 4. Wide scan, C 1s, and Br 3d core-level curve-fitted XPS spectra of the (a,b,b') PCL-*g*-P(GMA)1 from 1 h of ATRP reaction and (c,d,d') PCL-*g*-P(GMA)2 from 3 h of ATRP reaction. Successful grafting of P(GMA) polymer brushes can be deduced from the area ratios of [C-H]:[C-O]:[O=C-O] peak components comparable to the theoretical value of 3:3:1 of GMA molecular structure.

The grafting yield (GY) was measured to evaluate the kinetics of polymer chain growth in this study. As shown in Fig. 5, an approximate linear increase in GY of the grafted P(GMA) chains with polymerization time could be observed for the PCL-Br surface. The result suggests that the chain growth from the PCL-Br surface proceeds in a controlled and well-defined manner. The GY values of the PCL-*g*-P(GMA)1 and PCL-*g*-P(GMA)2 surfaces are about 6.31 ± 1.32 and 14.76 ± 2.63 μg/cm^2 (Table 1), respectively. The persistence of the Br 3d core-level signal (Figs. 4b' and 4d') is consistent with the fact that the living chain end from

http://dx.doi.org/10.5772/52646

the ATRP process involves a dormant alkyl halide group, which can be readily reactivated to initiate the block copolymerization [25]. However, the molecular weight and molecular weight distribution of the surface-graft polymers cannot be determined with sufficient accuracy without precise cleavage of the grafted P(GMA) from the film surfaces [27].

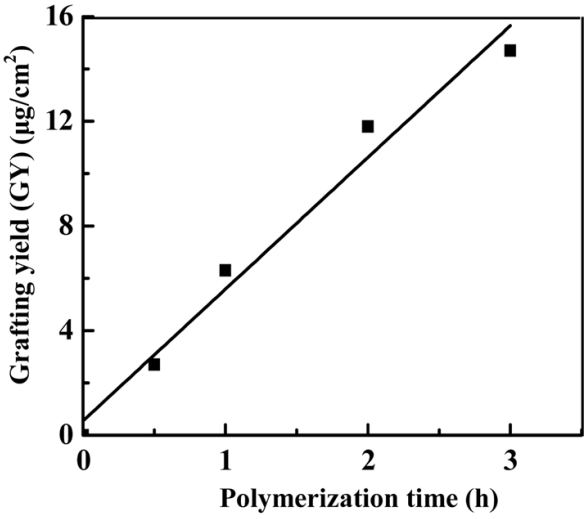

Figure 5. A linear relationship between the grafting yield (GY) of the P(GMA) brushes with the surface-initiated ATRP time. The polymer chain growth was tuneable by varying reaction time.

Nucleophilic reactions involving $-NH_2$ moieties of biomolecules and the pendant epoxide groups have been widely reported [44]. In this work, cell-adhesive gelatin was directly coupled to the pendant epoxide groups of the PCL-*g*-P(GMA)1 and PCL-*g*-P(GMA)2 surfaces to produce the corresponding PCL-*g*-P(GMA)1-*c*-gelatin and PCL-*g*-P(GMA)2-*c*-gelatin surfaces, respectively. Fig. 6 shows the respective wide scan, C 1s and N 1s core-level spectra of the gelatin-immobilized PCL surfaces. The corresponding curve-fitted C 1s core-level spectrum was composed of five peak components with BEs at about 284.6, 285.5, 286.2, 288.2 and 289.1 eV, attributable to the C-H, C-N, C-O, O=CNH, and O=C-O species [41], respectively (Figs. 6b and 6d). The C-N peak component is associated with the linkages in gelatin itself, as well as the linkage between P(GMA) and gelatin. The O=CNH peak component is ascribed to the peptide bonds in gelatin. The above results and the appearance of a strong N 1s signal with BE at 399.6 eV (Figs. 6b' and 6d'), characteristic of amine species, are consistent with the fact that gelatin has been covalently immobilized on the P(GMA) brushes. The surface wettability of the PCL substrates is significantly improved after the immobilization of gelatin, as water contact angles decrease to 37 ± 2° (for the PCL-*g*-P(GMA)1-*c*-gelatin) and 35 ± 3°(for the PCL-*g*-P(GMA)2-*c*-gelatin) (Table 1). It is reported that gelatin contains large amount of glycine (Gly) and proline (Pro) which are hydrophilic amino acids [45]. The hydroxyl groups (-OH) generated in the ring-opening reaction of epoxide groups by coupling

of gelatin could have also contributed to the lower water contact angle of the PCL-*g*-P(GMA)-*c*-gelatin surfaces.

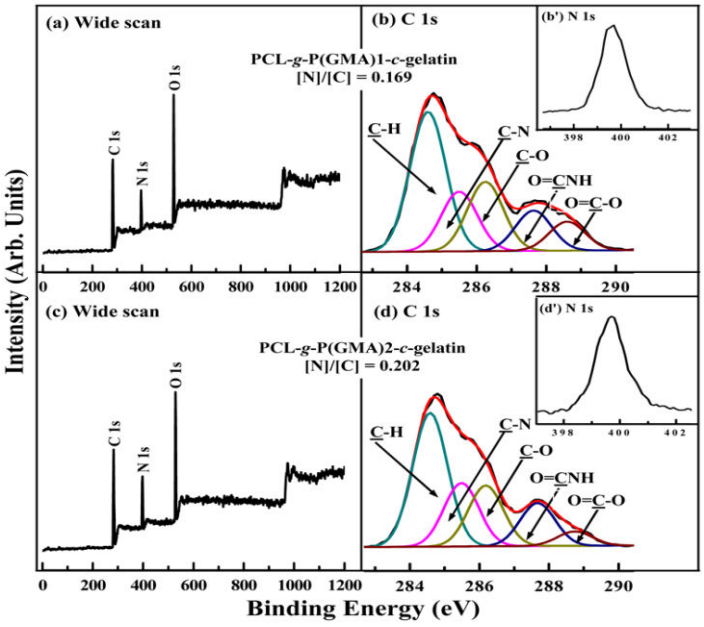

Figure 6. Wide scan, C 1s and N 1s core-level curve-fitted XPS spectra of the (a,b,b') PCL-*g*-P(GMA)1-*c*-gelatin and (c,d,d') PCL-*g*-P(GMA)2-*c*-gelatin surfaces. The appearance of two additional peak components of C-N and O=CNH as a result of immobilized gelatin.

3.3. Surface topography

The changes in topography of the PCL film surfaces after each functionalization step were investigated by AFM. Fig. 7 shows the representative AFM height images of the pristine PCL and functionalized PCL surfaces with scanned areas of 10 μm × 10 μm. The pristine PCL film surface is relatively uniform and smooth with a root-mean-square surface roughness values (R_a) of about 19 nm (Fig. 7a). After the aminolysis treatment, the R_a value increases to 31 nm (Fig. 7b). The observation that aminolysis caused a noticeable increase in surface roughness is in agreement with the findings by other groups [30,35]. The existence of shallow pits is probably the result of the penetration of hexanediamine molecules into the PCL films, since it has been previously reported that the aminolysis reaction can take place at a depth of around 50 μm [23,30]. After graft polymerization of GMA, obvious increases in R_a values are observed on the PCL-*g*-P(GMA)1 (56.9 nm, Fig. 7c) and PCL-*g*-P(GMA)2 surfaces (67.8 nm, Fig. 7e), and characteristic fiber-like features of polymer brushes are also visible on the P(GMA)-grafted film surfaces (Figs. 7c and 7e). The subsequent coupling of gelatin to P(GMA) brushes resulted in a further slight increase in surface roughness of PCL

http://dx.doi.org/10.5772/52646

substrates, as R_a values increase to 59 nm and 71.5 nm for the PCL-*g*-P(GMA)1-*c*-gelatin and the PCL-*g*-P(GMA)2-*c*-gelatin surfaces, respectively.

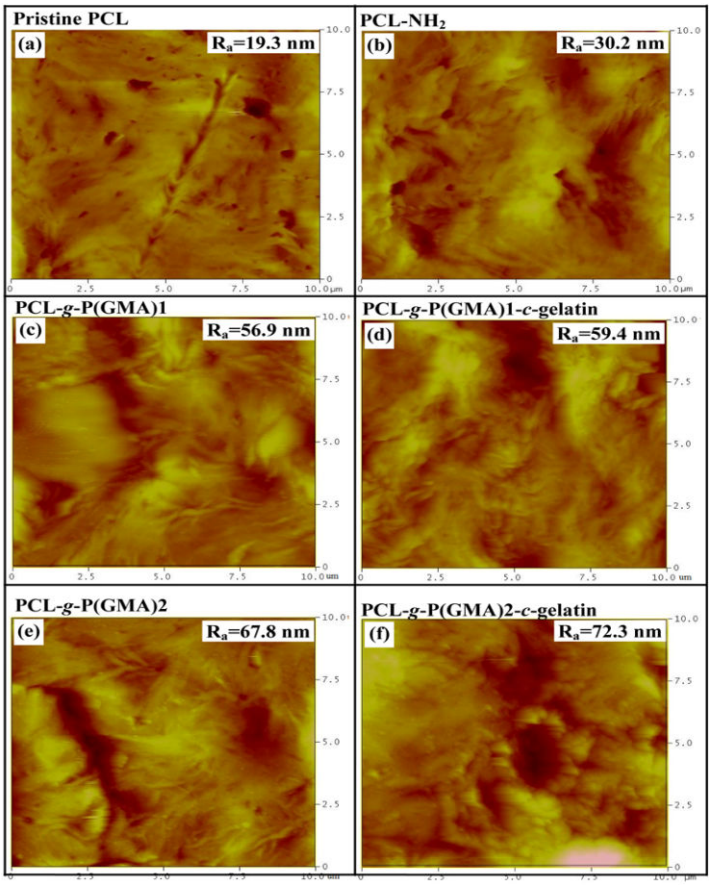

Figure 7. Representative two-dimensional (2D) AFM images of (a) pristine PCL, (b) PCL-NH_2, (c) PCL-*g*-P(GMA)1 from 1 h of ATRP, (d) PCL-*g*-P(GMA)2 from 3 h of ATRP, (e) PCL-*g*-P(GMA)1-*c*-gelatin, and (f) PCL-*g*-P(GMA)2-*c*-gelatin surfaces. The arithmetical mean roughness (R_a) of different PCL substrates was obtained from a scan size of 10 μm × 10 μm.

3.4. Endothelial cells proliferation and surface endothelialization

The adhesion and proliferation of endothelial cells (ECs) on the functionalized PCL surfaces was quantitatively determined by the AlamarBlueTM (AB) assay, and the results are shown in Fig. 8. The pristine PCL film surface is the least conducive for supporting cellular growth, since only a marginal increase in cells over 7 days of culture was observed. The cells attached to the PCL-NH_2 film surfaces showed a slight improvement in proliferation as compared to the pristine PCL surface. This result is consistent with previous findings that the presence

of amine groups on the PCL surfaces leads to a positive effect on cell proliferation [23,30], albeit to a limited extent. Despite the improvement in surface hydrophilicity and roughness, the grafting of P(GMA) brushes onto the PCL film surfaces did not lead to an enhancement in EC proliferation behavior, which is probably associated with the cytotoxicity and mutagenicity of epoxides groups to ECs [46]. Besides the fact that polymer surfaces with moderate hydrophilicity of water contact angles in a range of 30-70° and rougher nano-topography are favorable for cell attachment and proliferation [47,48], other factors (e.g. biological cues) may also be required for positive cell interaction with material substrates. This hypothesis was confirmed by the observation that the gelatinized P(GMA)-grafted PCL substrates exhibited higher affinity and proliferation for ECs as compared to the surfaces that did not contain the bioactive gelatin motifs.

In fact, the proliferation rates of the PCL-*g*-P(GMA)1-*c*-gelatin and PCL-*g*-P(GMA)2-*c*-gelatin surfaces were comparable to that of the gelatin-coated coverslips (positive controls). Cell proliferation on the gelatin-immobilized PCL surfaces was not only significantly enhanced, but also found to be positively correlated to the amounts of immobilized gelatin. The PCL-*g*-P(GMA)2-*c*-gelatin surface exhibited more pronounced enhancement in cell adhesion and proliferation than that of the PCL-*g*-P(GMA)1-*c*-gelatin surface, as the longer ATRP reaction time allowed for more gelatin to be attached. This result suggests that an increase in surface density of the immobilized gelatin can lead to an increase in EC proliferation over time. This phenomenon is probably associated with the fact that immobilization of gelatin provides many epitopes or ligands for cell adhesion molecules, such as integrins, thus mimicking the natural extracellular environment that is favorable for EC adhesion, spreading and proliferation.

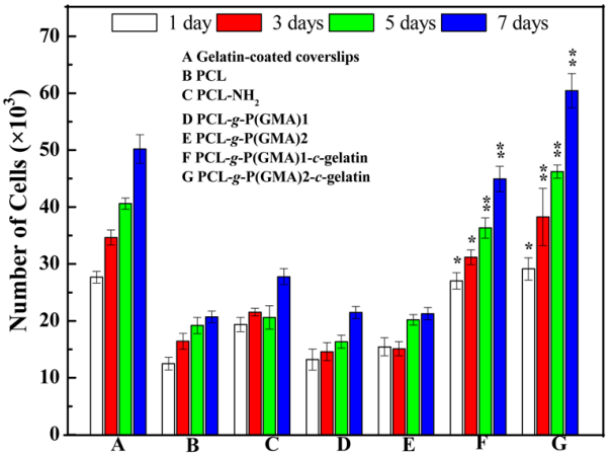

Figure 8. EC proliferation profile on the gelatin-coated coverslips, pristine PCL and functionalized PCL surfaces after 1, 3, 5 and 7 days of incubation at 37 °C in a 5% CO_2 atmosphere as determined by the AlamarBlue™(AB) assay. Data presented as means ± SD. *p<0.05 and **p<0.01 refers to statistically significant difference compared with the pristine PCL surface. The cell proliferation rate of ECs seeded on the gelatin-immobilized surfaces was significantly improved as compared to that the pristine PCL film.

http://dx.doi.org/10.5772/52646

The visualization of EC coverage on the functionalized PCL surfaces enabled a good assessment of the efficacy of endothelialization over the entire surface. Fig. 9 shows the representative fluorescence images of LIVE/DEAD-stained ECs on the pristine PCL and functionalized PCL film surfaces after 7 days of culture. The sparse coverage of ECs on the pristine PCL substrate further confirmed the unfavorable surface properties of pristine PCL for cell adhesion and proliferation (Fig. 9b). Poor endothelialization was also observed on the aminolyzed PCL (Fig. 9c) and P(GMA)-grafted PCL surfaces (Fig. 9d). The dense growth of ECs on the PCL-*g*-P(GMA)1-*c*-gelatin (Fig. 9e) and PCL-*g*-P(GMA)2-*c*-gelatin (Fig. 9f) surfaces indicated significant improvement in EC coverage for the gelatin-immobilized PCL surfaces. The observed denser coverage of ECs on the PCL-*g*-P(GMA)2-*c*-gelatin surfaces compared to the PCL-*g*-P(GMA)1-*c*-gelatin surfaces meant that the efficacy of endothelialization is positively correlated to the amount of immobilized gelatin. Taken together, the results suggest that the higher the surface concentration of immobilized gelatin, the better the endothelialization efficacy of the material within a given period of time.

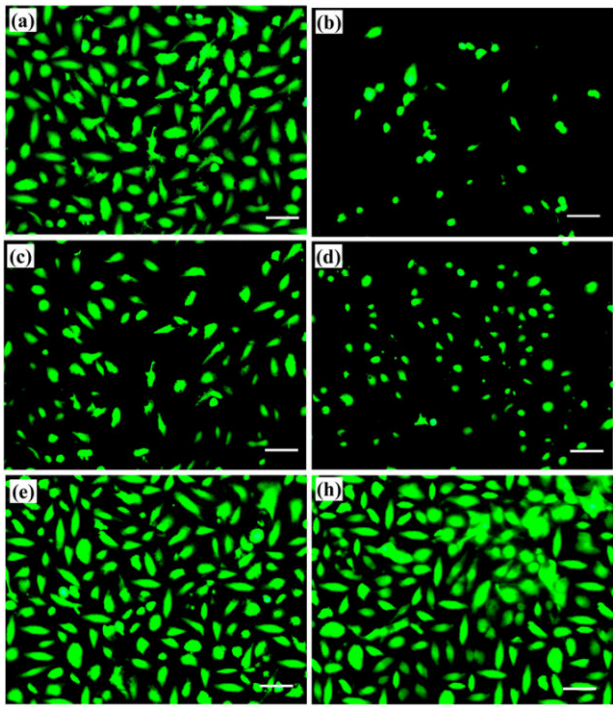

Figure 9. Fluorescence images of LIVE/DEAD-stained ECs on the (a) gelatin-coated coverslips (positive control), (b) pristine PCL, (c) PCL-NH_2, (d) PCL-*g*-P(GMA)2, (e) PCL-*g*-P(GMA)1-*c*-gelatin, and (f) PCL-*g*-P(GMA)2-*c*-gelatin after 7 days of incubation in cell suspension (2×10^4 cells/ml). Scale bar: 20 μm. Rapid endothelialization was observed for the gelatin-immobilized PCL surfaces.

3.5. Blood compatibility tests

3.5.1. Hemolysis rate test

Hemolysis rate is an important factor for characterization of the blood compatibility. The lower the hemolysis rate, the better the blood compatibility. Figure 10 shows the hemolysis rate of the pristine PCL and surface-functionalized PCL samples. It can be seen that the hemolysis rate of the functionalized samples has no substantial improvement. The gelatin-immobilized PCL substrates even show a relatively higher hemolysis rate than those of the pristine PCL and PCL-NH_2 surfaces. This result is consistent with the previous findings that gelatin exhibited somewhat hemostatic effect by nature. However, the hemolysis rate of the gelatin-immobilized PCL samples is approximately 3%, far below the accepted threshold value of 5% for biomaterial applications. Thus, the gelatin-immobilized samples can be used as a novel material with good hemocompatibility.

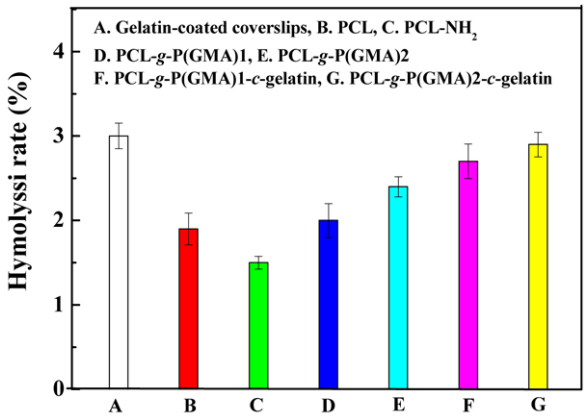

Figure 10. Hemolysis rate of the pristine PCL and surface-functionalized PCL samples. Data presented as means ± SD, n=3.

3.5.2. Coagulation activity on the bare and endothelialized PCL substrates

Blood coagulation, particularly under conditions of relatively low flow, has been recognized to be one of the main problems of vascular occlusion [49]. Activated coagulation factors influence the clotting time through extrinsic, intrinsic and common coagulation pathways. Prothrombin time (PT) is used to evaluate deficiencies in the extrinsic factor, and represents the time for blood plasma to clot after the addition of thromboplastin (activator of the extrinsic pathway) [50]. Activated partial thromboplastin time (APTT) is used to evaluate the intrinsic factors, such as VIII, IX, XI and XII, and common coagulation pathway factors V, X and II [50]. Both PT and APTT are commonly used to screen for adverse activation of the coagulation pathways on the vascular grafts and to evaluate their haemocompatibility in vi-

http://dx.doi.org/10.5772/52646

tro. Thus, the PT and APTT values of the bare and endothelialized PCL substrates with various surface modifications were measured.

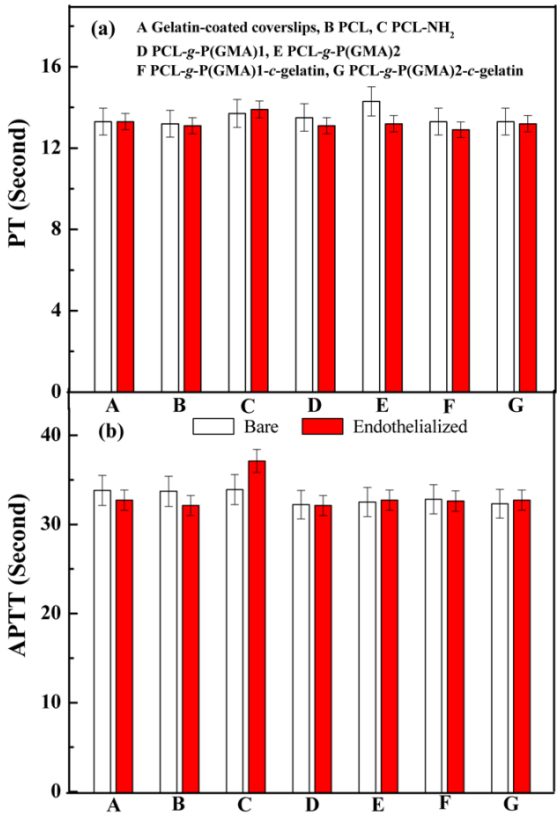

Figure 11. a) PT and (b) APTT results (means ± SD, n=3) for the bare and endothelialized surfaces of pristine PCL and surface-functionalized PCL, The coagulation activity of all surfaces was found to be in the normal range for healthy blood plasma.

The normal ranges of PT and APTT for healthy blood plasma are 12.0-14.5 s and 27.0-35.6 s, respectively [51]. Fig. 11 shows the PT and APTT results for the bare and endothelialized PCL substrates with various surface modifications. For the bare PCL and functionalized PCL surfaces, both PT and APTT are all within the normal ranges of coagulation time. None of the PCL substrates was found to affect the coagulation pathways significantly, and no discernible effect was observed in the presence of gelatin, indicating that surface functionalization activated neither the intrinsic nor the extrinsic coagulation pathways. This result is consistent with previous findings by other groups that cell-adhesive proteins and peptides do not affect or convert blood coagulation pathways [51,52]. Even after the PCL substrates were coated with a layer of ECs, the PT and APTT readings were still observed to be in the

normal range of the clinical reference, and no significant differences in the coagulant activities were observed on the endothelialized PCL substrates as compared to the bare PCL substrates. The results also revealed that the ECs cultured on the pristine PCL and functionalized PCL surfaces remained unactivated and did not exhibit procoagulation phenotypes. Hence, it could be concluded that the presence of the monolayer of ECs had no effect on the intrinsic or the extrinsic coagulation pathways.

3.5.3. Nitric Oxide (NO) production

Nitric oxide (NO) is an important regulator of vascular tone and platelet adhesion and the continuous NO release by ECs prevents thrombogenesis [53]. In this study, the NO secretion of the ECs on the pristine PCL and functionalized PCL surfaces were measured. As shown in Fig. 12, the amount of NO secreted by ECs on the gelatin-immobilized PCL surfaces was significantly higher than those on the pristine PCL, aminolyzed and P(GMA)-grafted PCL surfaces. The amount of NO production of the ECs seeded on the PCL-*g*-P(GMA)2-*c*-gelatin surface was around 2-fold higher than that on the PCL-*g*-P(GMA)1-*c*-gelatin surfaces, indicating that the improved NO production observed for ECs grown on the gelatin-immobilized PCL surface may be positively correlated to the amount of covalently immobilized gelatin. The above results suggest that a high density of immobilized gelatin led to the enhancement in NO secretion.

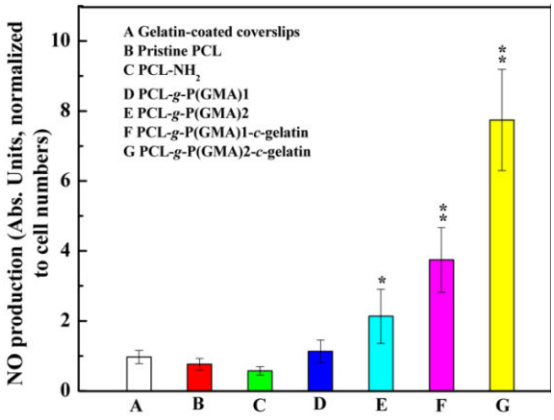

Figure 12. The amount of NO production for the ECs seeded on the pristine and functionalized PCL substrates. Data presented as means ± SD, n=3. *p<0.05 and **p<0.01 corresponds to statistically significant difference as compared to the pristine PCL.

3.5.4. Platelet activation on the bare and endothelialized PCL substrates

Apart from coagulation pathways, platelet activation is considered another important criterion in assessing blood compatibility of the biomaterial surface. The activation of attached platelet results in platelet aggregation and the formation of a thrombus [54]. The subendo-

http://dx.doi.org/10.5772/52646

thelial collagens (i.e., types I - IV) have been found to interact directly with platelets to trigger their activation for thrombogenic initiation [55]. As gelatin is a derivative of collagen, one downside of using gelatin-immobilized surfaces could be the detrimental adhesion and activation of platelets, which could initiate clotting. Therefore, the extent of platelet activation by the different biomaterial surfaces was studied.

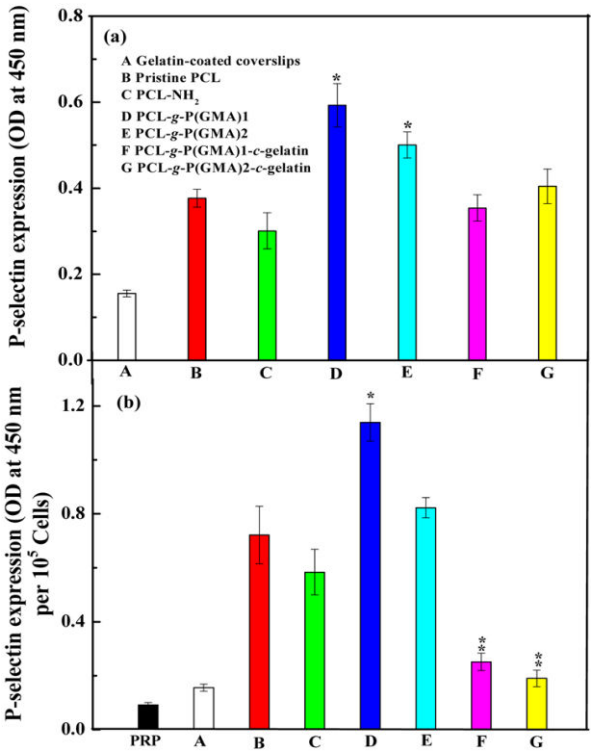

Figure 13. P-selectin expression for the (a) bare and (b) endothelialized surfaces of the pristine and functionalized PCL substrates. Plasma rich platelet (PRP) was used as positive control. *p<0.05 and **p<0.01 corresponds to statistically significant difference compared with the pristine PCL surface.

In this study, platelet activation on the bare and endothelialized PCL substrates was determined using the P-selectin assay, since P-selectin is one of intracellular granular molecules released upon platelet activation and stimulation [5], For the bare PCL substrates, the amount of activated platelets on the gelatin-immobilized PCL surfaces was comparable to those of the pristine PCL surfaces (Fig. 13a). In contrast, platelet activation was found to be significantly higher on the P(GMA)-grafted PCL surfaces, indicative of an increased risk for thrombogenesis. The results suggest that the immobilization of gelatin on the P(GMA)-grafted PCL surfaces not only rendered them with adhesion-promoting properties, but also decreased the risk of inducing the activation of platelets. It has been re-

ported previously that the biological motifs immobilized on the polymers could not bind effectively with the platelet integrin unless their separation distances was between 1.48-2.2 nm [56], and that polymers with small spacer, such as lauric acid-conjugated GRGDS, exhibited no increase in activation [57]. Here, the gelatin was directly conjugated onto the grafted P(GMA) brushes (small spacer), and thus the gelatin motif could not gain access to the binding sites of the platelet integrin (such as $\alpha 2\beta 1$). In addition, it is probable that the other surface properties (e.g. enhanced hydrophilicity) were also responsible for reduced platelet activation activity.

In the case of the endothelialized PCL substrates, the amount of activated platelets on the gelatin-immobilized PCL surfaces was significantly reduced with respect to the other endothelialized PCL substrates (Fig. 13b), indicative of good anti-thrombogenic behavior of the EC confluent layer. This result is consistent with the high level of NO production by ECs on the gelatinized PCL surface. The P-selectin expression on the endothelialized pristine PCL and PCL-NH_2 surfaces was higher than those on the bare substrates (Fig. 13b), which is line with the well-established fact that subconfluent EC layers were more thrombogenic in nature [13]. The platelet activation was significantly enhanced on the endothelialized P(GMA)-grafted PCL surfaces, as observed by the high levels of P-selectin expression, which is an indication of an increased risk of thrombogenesis for those surfaces. Overall, the above results showed that the thrombogenicity of a biomaterial is influenced by both EC confluency and the surface properties of the biomaterial. Consequently, it can be concluded that the immobilization of gelatin on the P(GMA) brushes prevented platelet activation, but that the presence of the P(GMA) brushes alone led to a pro-thrombogenic surface.

3.5.5. Expression and activity of vWF and MMP-2 of EC on the surface-functionalized PCL samples

In order to further investigate the thrombogenicity of endothelialized surfaces, we performed real-time PCR tests and protein immunoblotting on factors that mediate platelet adhesion to ECs. The expression of von Willebrand factor (vWF) on endothelial cells promotes platelet adhesion and high or abnormal expression of vWF has been implicated in pathological conditions such as thrombosis [58]. Matrix metalloproteinase-2 (MMP-2) is another factor known to be involved in platelet aggregation, as well as to have important roles in the degradation and remodeling of the endothelial extracellular matrix [59, 60]. 7 days after the seeding of ECs, the relative expression of both vWF and MMP-2 mRNA in the EC on both PCL-*g*-P(GMA)1-*c*-gelatin and PCL-*g*-P(GMA)2-*c*-gelatin surfaces were downregulated when compared to the ECs on PCL-*g*-P(GMA) surfaces and gelatin-coated coverslips (Fig. 14a and 14c). Immunoblotting of the vWF protein produced in ECs, also, suggest that it is lower in ECs on PCL-*g*-P(GMA)- *c*-gelatin surfaces in comparison to PCL-*g*-P(GMA) surfaces but differed where the vWF expression of ECs on the pristine PCL surface and gelatin-coated coverslip could not be detected (Fig. 14b). Nevertheless, these results suggest that pro-thrombogenic factors could be increased on bare PCL-*g*-P(GMA) surfaces and the conjugation of gelatin could help to reduce thrombogenicity.

http://dx.doi.org/10.5772/52646

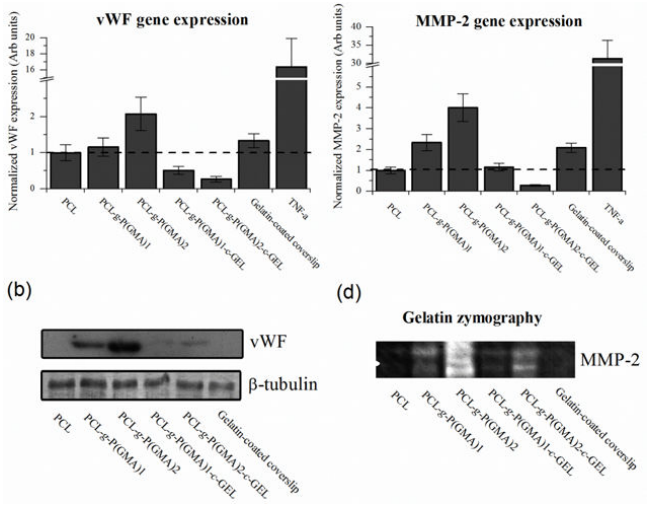

Figure 14. Real-time qPCR revealed that the expression of (a) vWF and (c) MMP-2 in ECs on PCL-*g*-P(GMA)-*c*-gelatin surfaces is lower when compared to PCL-*g*-P(GMA) surfaces and gelatin-coated coverslips. Expression levels are normalized using the housekeeping gene rpl27 and taken relative to ECs on pristine PCL (dotted line) (mean ± SD, n=3). Endothelial cells treated with TNF-αfor 6 h were used as a positive control for the expression of both genes. (c) Immunoblotting of vWF protein expressed in ECs on PCL-*g*-P(GMA)-*c*-gelatin is also reduced when compared to PCL-*g*-P(GMA) surfaces, thus corroborating the real-time PCR results.

4. Conclusion

This study described the successful biofunctionalization of PCL substrates with tunable surface densities of covalently-immobilized gelatin by surface-initiated ATRP of glycidyl methacrylate (GMA). Kinetics studies revealed that the grafting yield of the functional P(GMA) brushes increased linearly with polymerization time, and the amount of immobilized gelatin increased with the concentration of epoxide groups on the P(GMA) brushes. The significant improvement in the adhesion and proliferation of ECs on the gelatin-immobilized PCL substrates were found to be positively correlated to the amount of covalently immobilized gelatin. Blood compatibility tests demonstrated that the ECs cultured on the gelatin-immobilized-P(GMA) surfaces exhibited low platelet activation and significantly increased nitric oxide (NO) production, although the coagulation pathways were not affected both before and after EC coverage. Overall, the high surface-density of immobilized gelatin obtained by surface-initiated ATRP on the PCL surfaces is favorable for EC attachment and proliferation. The attached ECs maintained an unactivated and non-thrombogenic phenotype that mimics the EC lining of a healthy blood vessel. Hence, such a surface may have huge potential for vascular graft applications.

Acknowledgements

This research is supported by the Singapore National Research Foundation under CREATE programme: The Regenerative Medicine Initiative in Cardiac Restoration Therapy (NRF-Technion).

Author details

Shaojun Yuan[1,2*], Gordon Xiong[2], Ariel Roguin[3], Swee Hin Teoh[4] and Cleo Choong[2*]

*Address all correspondence to: yuanshaojun@gmail.com

*Address all correspondence to: cleochoong@ntu.edu.sg

1 Multi-phases Mass Transfer & Reaction Engineering Lab, College of Chemical Engineering, Sichuan University, Chengdu, China

2 School of Materials Science and Engineering, Nanyang Technological University, Singapore

3 Department of Cardiology, Rambam Medical Center, B. Rappaport Faculty of Medicine, Technion – Israel Institute of Technology, Israel

4 School of Chemical and Biomedical Engineering, Nanyang Technological University, Singapore

References

[1] Chlupac J, Filova E, Bacakova L. Blood vessel replacement: 50 years of development and tissue engineering paradigms in vascular surgery. *Physiol Res.* 2009;58:S119-S139.

[2] Mitchell SL, Niklason LE. Requirements for growing tissue-engineered vascular grafts. *Cardiovasc Pathol* 2003;12(2):59-64.

[3] Wang XW, Lin P, Yao QH, Chen CY. Development of small-diameter vascular grafts. *World J. Surg.* 2007;31(4):682-689.

[4] Sharkawi T, Darcos V, Vert M. Poly(DL-lactic acid) film surface modification with heparin for improving hemocompatibility of blood-contacting bioresorbable devices. *J. Biomed. Mater. Res. A* 2011;98A(1):80-87.

[5] Liu HF, Li XM, Niu XF, Zhou G, Li P, Fan YB. Improved hemocompatibility and endothelialization of vascular grafts by covalent immobilization of sulfated silk fibroin on poly(lactic-co-glycolic acid) scaffolds. *Biomacromolecules* 2011;12(8):2914-2924.

[6] Lee JH, Oh SH. MMA/MPEOMA/VSA copolymer as a novel blood-compatible material: Effect of PEO and negatively charged side chains on protein adsorption and platelet adhesion. *J. Biomed. Mater. Res.* 2002;60(1):44-52.

[7] Lee JH, Ju YM, Kim DM. Platelet adhesion onto segmented polyurethane film surfaces modified by addition and crosslinking of PEO-containing block copolymers. *Biomaterials* 2000;21(7):683-691.

[8] Amiji M, Park K. Surface modification of polymeric biomaterials with poly(ethylene oxide), albumin and heparin for reduced thrombogenicity. *J Biomater Sci-Polym Ed* 1993;4(3):217-234.

[9] Chong MSK, Teoh SH, Teo EY, Zhang ZY, Lee CN, Koh S, Choolani M, Chan J. Beyond cell capture: antibody conjugation improves hemocompatibility for vascular tissue engineering applications. *Tissue Eng. Part A* 2010;16(8):2485-2495.

[10] Ku SH, Park CB. Human endothelial cell growth on mussel-inspired nanofiber scaffold for vascular tissue engineering. *Biomaterials* 2010;31(36):9431-9437.

[11] Wu KK, Thiagarajan P. Role of endothelium in thrombosis and hemostasis. *Annu Rev Med* 1996;47:315-331.

[12] Lijnen HR, Collen D. Endothelium in hemostasis and thrombosis. *Prog. Cardiovasc. Dis* 1997;39(4):343-350.

[13] McGuigan AP, Sefton MV. The influence of biomaterials on endothelial cell thrombogenicity. *Biomaterials* 2007;28(16):2547-2571.

[14] Woodruff MA, Hutmacher DW. The return of a forgotten polymer - polycaprolactone in the 21st century. *Prog. Polym.Sci.* 2010;35(10):1217-1256.

[15] Sung HJ, Meredith C, Johnson C, Galis ZS. The effect of scaffold degradation rate on three-dimensional cell growth and angiogenesis. *Biomaterials* 2004;25(26):5735-5742.

[16] Chong MSK, Chan J, Choolani M, Lee CN, Teoh SH. Development of cell-selective films for layered co-culturing of vascular progenitor cells. *Biomaterials* 2009;30(12): 2241-2251.

[17] Serrano MC, Portoles MT, Vallet-Regi M, Izquierdo I, Galletti L, Comas JV, Pagani R. Vascular endothelial and smooth muscle cell culture on NaOH-treated poly (epsilon-caprolactone) films: A preliminary study for vascular graft development. *Macromol Biosci* 2005;5(5):415-423.

[18] de Valence S, Tille JC, Mugnai D, Mrowczynski W, Gurny R, Moller M, Walpoth BH. Long term performance of polycaprolactone vascular grafts in a rat abdominal aorta replacement model. *Biomaterials* 2012;33(1):38-47.

[19] Tillman BW, Yazdani SK, Lee SJ, Geary RL, Atala A, Yoo JJ. The in vivo stability of electrospun polycaprolactone-collagen scaffolds in vascular reconstruction. *Biomaterials* 2009;30(4):583-588.

[20] Walpoth BH, Moller M. Tissue engineering of vascular prostheses. *Chirurg* 2011;82(4):303-310.

[21] Serrano MC, Pagani R, Pena J, Vallet-Regi M, Comas JV, Portoles MT. Progenitor-derived endothelial cell response, platelet reactivity and haemocompatibility parameters indicate the potential of NaOH-treated polycaprolactone for vascular tissue engineering. *J Tissue Eng Regen Med* 2011;5(3):238-247.

[22] Ma ZW, Gao CY, Gong YH, Shen JC. Chondrocyte behaviors on poly-L-lactic acid (PLLA) membranes containing hydroxyl, amide or carboxyl groups. *Biomaterials* 2003;24(21):3725-3730.

[23] Zhu YB, Gao CY, Liu YX, Shen JC. Endothelial cell functions in vitro cultured on poly(L-lactic acid) membranes modified with different methods. *J. Biomed. Mater. Res. A* 2004;69A(3):436-443.

[24] Shin YM, Kim KS, Lim YM, Nho YC, Shin H. Modulation of spreading, proliferation, and differentiation of human mesenchymal stem cells on gelatin- immobilized poly(L-lactide-co-epsilon-caprolactone) substrates. *Biomacromolecules* 2008;9(7): 1772-1781.

[25] Edmondson S, Osborne VL, Huck WTS. Polymer brushes via surface-initiated polymerizations. *Chem Soc Rev* 2004;33(1):14-22.

[26] Coessens V, Pintauer T, Matyjaszewski K. Functional polymers by atom transfer radical polymerization. *Prog. Polym.Sci.* 2001;26(3):337-377.

[27] Xu FJ, Yang XC, Li CY, Yang WT. Functionalized polylactide film surfaces via surface-initiated ATRP. *Macromolecules* 2011;44(7):2371-2377.

[28] Jiang H, Wang XB, Li CY, Li JS, Xu FJ, Mao C, Yang WT, Shen J. Improvement of hemocompatibility of polycaprolactone film surfaces with zwitterionic polymer brushes. *Langmuir* 2011;27(18):11575-11581.

[29] Tiaw KS, Teoh SH, Chen R, Hong MH. Processing methods of ultrathin poly(epsilon-caprolactone) films for tissue engineering applications. *Biomacromolecules* 2007;8(3): 807-816.

[30] Zhu YB, Gao CY, Liu XY, Shen JC. Surface modification of polycaprolactone membrane via aminolysis and biomacromolecule immobilization for promoting cytocompatibility of human endothelial cells. *Biomacromolecules* 2002;3(6):1312-1319.

[31] Causa F, Battista E, Della Moglie R, Guarnieri D, Iannone M, Netti PA. Surface investigation on biomimetic materials to control cell adhesion: the case of RGD conjugation on PCL. *Langmuir* 2010;26(12):9875-9884.

[32] Yuan SJ, Wan D, Liang B, Pehkonen SO, Ting YP, Neoh KG, Kang ET: Lysozyme-coupled poly(poly(ethylene glycol) methacrylate)-stainless steel hybrids and their antifouling and antibacterial surfaces. *Langmuir* 2011;27(6):2761-2774.

[33] Zhu YB, Gao CY, Shen JC. Surface modification of polycaprolactone with poly(methacrylic acid) and gelatin covalent immobilization for promoting its cytocompatibility. *Biomaterials* 2002;23(24):4889-4895.

[34] Chang KY, Hung LH, Chu IM, Ko CS, Lee YD. The application of type II collagen and chondroitin sulfate grafted PCL porous scaffold in cartilage tissue engineering. *J. Biomed. Mater. Res. A* 2010;92A(2):712-723.

[35] Zhang HN, Hollister S. Comparison of bone marrow stromal cell behaviors on poly(caprolactone) with or without surface modification: studies on cell adhesion, survival and proliferation. *J Biomater Sci-Polym Ed* 2009;20(14):1975-1993.

[36] Gabriel M, Amerongen GV, Van Hinsbergh VWM, Amerongen AVV, Zentner A. Direct grafting of RGD-motif-containing peptide on the surface of polycaprolactone films. *J Biomater Sci-Polym Ed* 2006;17(5):567-577.

[37] von Burkersroda F, Schedl L, Gopferich A. Why degradable polymers undergo surface erosion or bulk erosion. *Biomaterials* 2002;23(21):4221-4231.

[38] Bech L, Meylheuc T, Lepoittevin B, Roger P. Chemical surface modification of poly(ethylene terephthalate) fibers by aminolysis and grafting of carbohydrates. *J. Polym Sci Pol Chem* 2007;45(11):2172-2183.

[39] Moulder J F, Sobol FE, Bomben KD. Handbook of X-ray photoelectron spectroscopy. Eden Prairie, Minn: Perkin-Elmer Corp.; 1992.

[40] Siegwart DJ, Oh JK, Matyjaszewski K. ATRP in the design of functional materials for biomedical applications. *Prog. Polym.Sci.* 2012;37(1):18-37.

[41] Xu FJ, Cai QJ, Li YL, Kang ET, Neoh KG. Covalent immobilization of glucose oxidase on well-defined poly(glycidyl methacrylate)-Si(111) hybrids from surface-initiated atom-transfer radical polymerization. *Biomacromolecules* 2005;6(2):1012-1020.

[42] Chan K, Gleason KK. Photoinitiated chemical vapor deposition of polymeric thin films using a volatile photoinitiator. *Langmuir* 2005;21(25):11773-11779.

[43] Wang T, Kang ET, Neoh KG, Tan KL, Cui CQ, Lim TB. Surface structure and adhesion enhancement of poly(tetrafluooethylene) films after modification by graft copolymerization with glycidyl methacrylate .*J. Adhes. Sci. Technol.* 1997;11(5):679-693.

[44] Eckert AW, Grobe D, Rothe U. Surface-modification of polystyrene-microtitre plates via grafting of glycidylmethacrylate and coating of poly-glycidylmethacrylate. *Biomaterials* 2000;21(5):441-447.

[45] Xia Y, Boey F, Venkatraman SS. Surface modification of poly(L-lactic acid) with biomolecules to promote endothelialization. *Biointerphases* 2010;5(3):FA32-FA40.

[46] Marquard H, Selkirk JK, Sims P, Kuroki T, Heidelbe C, Huberman E, Grover PL. Malignant transformation of cells derived from mouse prostate by epoxide and other derivatives of polycylic hydrocarbons. *Cancer Res* 1972;32(4):716-720.

[47] Cheng ZY, Teoh SH. Surface modification of ultra thin poly(ε-caprolactone) films using acrylic acid and collagen. *Biomaterials* 2004;25(11):1991-2001.

[48] Arima Y, Iwata H. Effect of wettability and surface functional groups on protein adsorption and cell adhesion using well-defined mixed self-assembled monolayers. *Biomaterials* 2007;28(20):3074-3082.

[49] van der Zijpp YJT, Poot AA, Feijen J. ICAM-1 and VCAM-1 expression by endothelial cells grown on fibronectin-coated TCPS and PS. *J. Biomed. Mater. Res. A* 2003; 65A(1):51-59.

[50] Kamal AH, Tefferi A, Pruthi RK. How to interpret and pursue an abnormal prothrombin time, activated partial thromboplastin time, and bleeding time in adults. *Mayo Clin Proc* 2007;82(7):864-873.

[51] Liu YA, Wang W, Wang J, Wang YL, Yuan Z, Tang SM, Liu M, Tang H. Blood compatibility evaluation of poly(D,L-lactide-co-beta-malic acid) modified with the GRGDS sequence. *Colloid Surf B-Biointerfaces* 2010;75(1):370-376.

[52] Hansson KM, Tosatti S, Isaksson J, Wettero J, Textor M, Lindahl TL, Tengvall P. Whole blood coagulation on protein adsorption-resistant PEG and peptide functionalised PEG-coated titanium surfaces. *Biomaterials* 2005;26(8):861-872.

[53] Graves JE, Greenwood IA, Large WA. Tonic regulation of vascular tone by nitric oxide and chloride ions in rat isolated small coronary arteries. *Am J Physiol-Heart Circul Physiol* 2000;279(6):H2604-H2611.

[54] Allen RD, Zacharski LR, Widirstky ST, Rosenstein R, Zaitlin LM, Burgess DR. Transformation and motility of human-platelets - details of the shape change and release reaction observed by optical and electron-microscopy. *J Cell Biol* 1979;83(1):126-142.

[55] Saelman EUM, Nieuwenhuis HK, Hese KM, Degroot PG, Heijnen HFG, Sage EH, Williams S, McKeown L, Gralnick HR, Sixma JJ. Platelet-adhesion to collagen type-I through type-VIII under condtions of stasis and flow is mediated by $\alpha 2\beta 1$-integrin. *Blood* 1994;83(5):1244-1250.

[56] Hu B, Finsinger D, Peter K, Guttenberg Z, Barmann M, Kessler I, Escherich A, Moroder L, Bohm J, Baumeister W, Sui SF. Intervesicle cross-linking with integrin alpha(IIb)beta(3) and cyclic-RGD-lipopeptide. A model of cell-adhesion processes. *Biochemistry* 2000;39(40):12284-12294.

[57] Kidane AG, Punshon G, Salacinski HJ, Ramesh B, Dooley A, Olbrich M, Heitz J, Hamilton G, Seifalian AM. Incorporation of a lauric acid-conjugated GRGDS peptide directly into the matrix of a poly(carbonate-urea)urethane polymer for use in cardiovascular bypass graft applications. *J. Biomed. Mater. Res. A* 2006;79A(3):606-617.

[58] Brill A, Fuchs TA, Chauhan AK, Yang JJ, De Meyer SF, Köllnberger M, et al. von Willebrand factor–mediated platelet adhesion is critical for deep vein thrombosis in mouse models. Blood. 2011; 117(4):1400-1407.

http://dx.doi.org/10.5772/52646

[59] Kazes I, Elalamy I, Sraer J-D, Hatmi M, Nguyen G. Platelet release of trimolecular complex components MT1-MMP/TIMP2/MMP2: involvement in MMP2 activation and platelet aggregation. Blood. 2000; 96(9):3064 –3069.

[60] Ben-Yosef Y, Lahat N, Shapiro S, Bitterman H, Miller A. Regulation of endothelial matrix metalloproteinase-2 by hypoxia/reoxygenation. Circulation Research. 2002; 90(7):784 –791.